Computer-Aided Bleeding Detection in WCE Video

Yanan Fu, *Student Member, IEEE*, Wei Zhang, *Member, IEEE*, Mrinal Mandal, *Senior Member, IEEE*, and Max Q.-H. Meng, *Fellow, IEEE*

***Abstract*—Wireless capsule endoscopy (WCE) can directly take digital images in the gastrointestinal tract of a patient. It has opened a new chapter in small intestine examination. However, a major problem associated with this technology is that too many images need to be manually examined by clinicians. Currently, there is no standard for capsule endoscopy image interpretation and classification. Most state-of-the-art CAD methods often suffer from poor performance, high computational cost, or multiple empirical thresholds. In this paper, a new method for rapid bleeding detection in the WCE video is proposed. We group pixels through superpixel segmentation to reduce the computational complexity while maintaining high diagnostic accuracy. Feature of each superpixel is extracted using the red ratio in RGB space and fed into support vector machine for classification. Also, the influence of edge pixels has been removed in this paper. Comparative experiments show that our algorithm is superior to the existing methods in terms of sensitivity, specificity, and accuracy.**

***Index Terms*—Bleeding detection, superpixel, wireless capsule endoscopy (WCE).**

I. Introduction

THE wireless capsule endoscopy (WCE), which first appeared in [1], uses an imaging capsule to view the whole gastrointestinal (GI) tract. The entire small intestine can be examined by this technique without pain, sedation, or air insufflation, which are inevitable in traditional endoscopy examination [2]. WCE obtained approval from the U.S. Food and Drug Administration in August 2001 for the purpose of "visualization of the small bowel mucosa as a tool in the detection of abnormalities of the small bowel."

The development of WCE has opened a new chapter in small intestine examination. More than one million PillCam video capsules have helped clinicians evaluate patients for GI disorders since Given Imaging Ltd. produced WCE. Based on WCE of the GI tract, clinicians are now able to detect severe diseases in early development states [3].

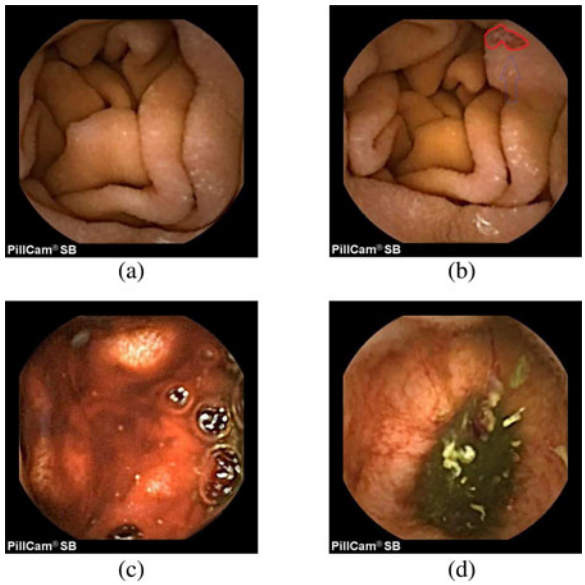

Fig. 1. WCE samples. (a) Normal image. (b) Bleeding caused by angiodysplasia. (c) Active bleeding. (d) Bleeding caused by ulcers.

As the most common indication for WCE, the obscure GI bleeding is defined as "bleeding of unknown origin that persists, or recurs, or is visible after a negative colonoscopy and/or upper endoscopy result" [4]. It is an important syndrome or group of symptoms rather than a single pathology for variety of small intestinal diseases, such as angiodysplasia, active bleeding, vascular lesions, tumor, ulcers, polyps, and Crohn's disease. Therefore, bleeding region detection in the WCE video can assist the clinicians to detect intestinal diseases.

As shown in Fig. 1(a), the normal intestine in WCE images generally has pinkish to yellowish color. Fig. 1(b)–(d) shows images with bleeding regions. More specifically, the bleeding in Fig. 1(b) is caused by angiodysplasia. Fig. 1(c) shows an active bleeding image. The bleeding in Fig. 1(d) is caused by ulcers. Apparently, bleeding will turn the tissue to be red. The hue of bleeding regions appears more reddish compared to the nonbleeding regions.

A WCE video normally contains around 57 000 images, which makes it a hard task to examine. Therefore, computer aided detection (CAD) method is very helpful to clinician in diagnosis [5]–[7]. However, currently, there is no standard for WCE image interpretation and classification. The suspected blood indicator designed by Given Imaging Ltd. can only detect the active bleeding regions in small intestine such as in Fig. 1(c). Also, this software is known to have insufficient sensitivity and specificity [8]. Recently, bleeding detection has received much

Manuscript received September 2, 2012; revised November 26, 2012 and February 28, 2013; accepted March 11, 2013. Date of publication April 12, 2013; date of current version March 3, 2014. This work was supported by the National Science Foundation of China (NSFC) under Grant 61203253.

Y. Fu and W. Zhang are with the School of Control Science and Engineering, Shandong University, Jinan 250061, China (e-mail: fyasdu@gmail.com; davidzhang@sdu.edu.cn).

M. Mandal is with the Department of Electrical and Computer Engineering, University of Alberta, Edmonton, AB T6G 2V4, Canada (e-mail: mmandal@ualberta.ca).

M. Q.-H. Meng is with the Department of Electronic Engineering, Chinese University of Hong Kong, Hong Kong (e-mail: max@ee.cuhk.edu.hk).

Color versions of one or more of the figures in this paper are available online at http://ieeexplore.ieee.org.

Digital Object Identifier 10.1109/JBHI.2013.2257819

attention. The existing methods can be roughly classified into image based methods, pixel based methods, and patch based methods [9].

Image based methods: Boulougoura *et al.* [10] proposed to detect bleeding regions using 54 statistical features (e.g., standard deviation, variance, and skew), calculated from a color histogram of six color components such as R, G, B, H, S, and V. Liu and Yuan [11] divided the WCE image into several blocks and kept only the intensity value of each block center. Finally, all intensity values were combined to form a feature vector for classification. Coimbra and Cunha [12] used MPEG-7 visual descriptors to detect three main abnormalities (bleeding, polyp, and tumor) in the GI tract. Other image based methods [13]–[17] work similarly but use different features or classifiers to detect bleeding regions. Image based methods process the image as a whole and often fail in small bleeding region detection. To summarize, image based methods are fast. However, the performance is often poor.

Pixel based methods: Recently, a fair amount of pixel based detection methods have been proposed. Pan *et al.* [18] proposed to detect bleeding pixels by using probabilistic neural network (PNN). Al-Rahayfeh and Abuzneid [19] distinguished the bleeding and nonbleeding pixels by thresholding in RGB and HSV color spaces, while Hwang *et al.* [20] used expectation maximization clustering method, and R, G, and B color features are used to produce the maximum likelihood estimates. Other similar methods can be found in [21]–[23]. Since the intensities bleeding and nonbleeding pixels often have overlapping in each color channel, thresholding methods are unreliable. The other methods classifying at pixel level work better but suffer from high computational cost.

Patch based methods: To achieve a tradeoff between accuracy and speed, Li and Meng [24] proposed a patch based method based on chrominance moments combined with local binary pattern (LBP) texture features. Each WCE image is divided into 64 patches and the 36 most informative patches are classified by multilayer perception (MLP) neural network. This method achieved high sensitivity but has low specificity and accuracy. Also, the shape, location, and size of each bleeding region varies much. But they divide every image into blocks uniformly and cannot deal with the boundary patches. Moreover, MLP is often evolved from linear perception and thus is unsuitable for the nonlinear pattern recognition problem.

In this paper, we propose a new method that can detect bleeding regions from WCE video more effectively and efficiently. Since edge pixels and bleeding pixels share similar hue, traditional algorithms often mistake edge pixels for bleeding pixels. We first detect the edge pixels, and then use the morphological dilation to locate and remove the edge regions. Instead of processing each pixel or dividing the image uniformly, we group pixels adaptively based on color and location through superpixel segmentation. Thus, each image can be represented by hundreds of superpixels and the computational complexity is also reasonable. For each superpixel, the feature is defined using the red ratio in RGB color space. Finally, support vector machine (SVM) is used to classify the bleeding and nonbleeding superpixels. Experimental results show that the proposed method has low computational complexity and maintains high performance as pixel based method.

Algorithm 1 The proposed framework

Input: WCE frame
1: Use canny detector to find the edge pixels.
2: Use morphological dilation to obtain edge regions.
3: Remove the edge regions by masking.
4: Group pixels with similar color and location by superpixel segmentation.
5: Classify superpixels based on color features by SVM.
Output: Bleeding or not (bleeding region segments)

Algorithm 2 Edge removal

1: Convert the WCE image from RGB space to CIELab space. For the L channel:
2: Detect the edge pixels using canny detector.
3: Use morphological method to dilate the detected edge regions.
4: Locate the edge regions by masking, i.e., the intensities of pixels in the edge regions are set to zeros.

II. Algorithm

As shown in Algorithm 1, the proposed method mainly consists of three steps: (1) image preprocessing; (2) superpixel segmentation; and (3) bleeding detection. The details are given in the following three sections.

A. Image Preprocessing

It is known that majority of false bleeding detections are caused by the edge regions [25], which are mainly caused by intestinal folds or camera defocus. Since edge pixels share similar hue as bleeding pixels, they are often mistaken for bleeding pixels. Hence, they should be removed before bleeding detection. The algorithm of edge removal is shown in Algorithm 2.

The contrast is the difference in visual properties that makes an object distinguishable from other objects and the background. In a typical WCE image, the most distinguishable feature between edge pixels and other nonbleeding pixels is the luminance. The bleeding pixels and nonbleeding pixels (except edge pixels) normally have similar luminance and differ in redness. Therefore, we perform the canny detector in the luminance L channel to find the edge pixels and most bleeding pixels can survive. Canny detector [26] is adopted to find edge pixels because it is fast and suitable for real-time detection.

After edge detection, edges are dilated to locate the edge regions using morphological operation. In detail, the dilation operator needs two inputs as shown in Eq. (1). A is the image to be dilated. B is a set of coordinate points known as a structuring element (also known as a kernel) which determines the precise

Algorithm 3 Superpixel segmentation

1: Use Gaussian filter to reduce the noise of WCE image.
2: Place K seeds $C_k = [l_k, a_k, b_k, x_k, y_k]$ by sampling the image with distance d.
3: **for** each pixel **do**
4: Label this pixel based on the seed that has closest similarity to it.
5: **end for**
6: Relabel the disjoint clusters and generate new superpixels.

effect of the dilation on the input image

$$A \oplus B = \{z | B_z \cap A \neq \emptyset\}. \quad (1)$$

This equation is based on obtaining the reflection of B about its origin and shifting this reflection by z. The dilation of A by B then is the set of all displacements, z, such that B and A overlap by at least one pixel. More details can be found in [27]. Finally, we obtain an image with enlarged edge regions which will be removed by masking as shown in Fig. 4(c).

B. Superpixel Segmentation

With the development of imaging technology, the resolution of sensor becomes higher and higher. The new generation WCE, PillCam SB2, captures nearly twice the mucosal area per image compared to PillCam SB, which makes the pixel by pixel methods more time consuming than before. To reduce the computational cost and make bleeding detection faster, we propose to group the pixels based on color and location first, and then detect bleeding at superpixel level.

As a restricted form of region segmentation, superpixels can balance the conflicting goals of reducing image complexity through pixel grouping while avoiding undersegmentation [28], [29]. Most superpixel methods often suffer from high computational cost, poor segmentation quality, inconsistent size and shape, or multiple difficult-to-tune parameters. In this section, we introduce an initial seed (cluster center) growth based approach extended from [29] and [30]. To limit the computational load of superpixel segmentation, we made several improvements for speeding up. Our method relies on pixel similarity to find clusters instead of using curve evolution, and thus works much faster than [29]. Our method maintains the simple linear clustering manner as [30] but has some new properties. First, since WCE images are often noisy because of the poor illumination conditions, we first use Gaussian filter to remove noise. Second, bleeding regions may be small in WCE image and appear as disjoint segments. To enforce connectivity, most methods relabel them with the labels of the larger neighboring cluster which may be a normal region. Thus, it is hard to detect bleeding from this superpixel since most pixels are nonbleeding. To remedy this problem, we assign a new label to the disjoint segment, and thus the small bleeding region can show up as a single superpixel. Besides, we found that one time segmentation can generate satisfied superpixel results for WCE images. So our algorithm is noniterative and thus is faster than [30]. The details are as follows:

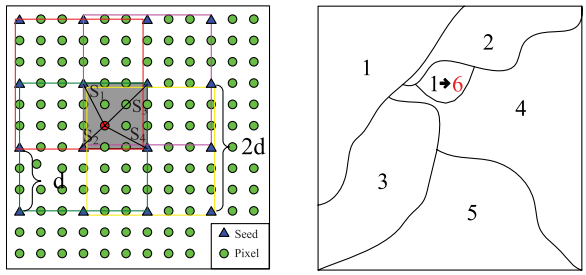

Fig. 2. Superpixel segmentation. (a) Similarity calculation. (b) Disjoint superpixel relabel.

As most previous methods, we place K seeds in a lattice formation to make the superpixels evenly distributed over the image. The distances between lattice neighbors are all approximately equal to d, where d is $\sqrt{\frac{N}{K}}$. N is the total number of pixels in an image.

The color similarity between pixels can be measured in the CIELab space as uniform changes of components in CIELab correspond to uniform changes in perceived color. The relative perceptual differences between any two colors in CIELab can be approximated by treating each color as a point in a 3-D space (with three components: l, a, b) and taking the Euclidean distance between them

$$S_{\text{color}} = \sqrt{(l_i - l_j)^2 + (a_i - a_j)^2 + (b_i - b_j)^2}. \quad (2)$$

Similarity of two pixels is not only related to the color similarity, but also related to the spatial distance as follows:

$$S_{\text{spatial}} = \sqrt{(x_i - x_j)^2 + (y_i - y_j)^2}. \quad (3)$$

Hence, we define the similarity measure S by combining them together as

$$S = S_{\text{color}} + \lambda \times S_{\text{spatial}} \quad (4)$$

where S_{color} is the color similarity in the CIELab space and S_{spatial} denotes the spatial distance between two pixels. (x, y) denotes the position of a pixel. The parameter λ is used to balance the contributions of color similarity and spatial distance.

As shown in Fig. 2(a), the K superpixel seeds are placed with sampling intervals d. Thus, to ensure enough overlapping, the searching space for each seed is set to $2d \times 2d$. Hence, pixels will be covered by its neighboring four seeds, and the similarity between each pixel and the four seeds should be calculated. Finally, each pixel will be associated with the seed that has the closest similarity to it.

However, there may exist a few disjoint segments in the result because the connectivity constraint of the same superpixel is not imposed. This may occur especially for bleeding regions because they are often small in the WCE image. Traditional methods will combine the disjoint segments with the neighboring segment to enforce connectivity. This may cause the bleeding region mixed with a nonbleeding region and thus this superpixel will be hard to differentiate. To avoid this, we assign a new label to each disjoint segment to ensure small region can

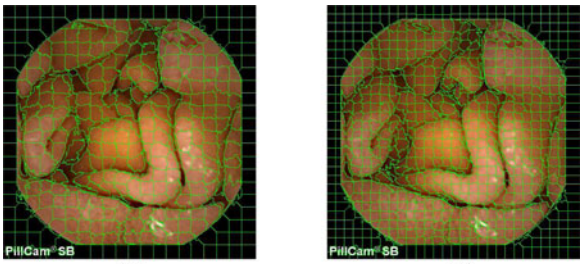

Fig. 3. Superpixel segmentation with different K. (a) $K = 400$. (b) $K = 800$.

show up as a single superpixel as shown in Fig. 2(b). The final segmentation results with different values of seed number K are shown in Fig. 3.

C. Superpixel Classification

Next, we will use SVM to train a classifier and detect bleeding superpixel by superpixel for each WCE image. The SVM package LIBSVM [31] is used to classify the bleeding and nonbleeding patterns. It is known that color is the most effective clue for clinicians to examine the GI tract. Bleeding occurs in the presence of red or dark red regions. Hence, the features we used for classifier training are mainly based on the RGB colors. As shown in Eq. (5), we define the feature vector $[F1, F2, F3]$ for each superpixel based on red ratio

$$\begin{aligned} F_1 &= R(i)/G(i) \\ F_2 &= R(i)/B(i) \\ F_3 &= R(i)/(R(i)+G(i)+B(i)) \end{aligned} \tag{5}$$

where R, G, B are the mean value of pixels in the i_{th} superpixel. It is worth noting that F_3 can also be referred as the chromaticity coordinate. It implies the relative proportion of R in the three channels, and can remove the ambiguity of brightness [32].

In the training process, 20 000 bleeding pixels and 40 000 nonbleeding pixels are selected to form a training set. So the training dataset contains 60 000 feature vectors and each vector has three red ratio features. The tenfold cross-validation and grid search based tool are used to train the optimal SVM classifier. For each WCE frame to be examined, all superpixels are checked with this classifier. If the image contains one or multiple bleeding superpixels, it is regarded as bleeding and should be shown to the clinicians. Otherwise, it is a normal frame and can be passed.

III. Experimental Results and Discussions

In the experiments, a set of 5000 WCE images consisting of 1000 bleeding frames and 4000 nonbleeding frames extracted from 20 different videos is tested for comparative evaluation. The images were already labeled by experienced clinicians. The image containing bleeding region was labeled as a positive sample. Otherwise, it was labeled as a negative sample. In this paper, the following parameters need to be set manually: the parameters in canny edge detection (standard deviation of the Gaussian function σ and sensitivity threshold T), the size of structural elements B in dilation, the superpixel number K, and balance parameter between color and spatial proximity λ in superpixel segmentation. However, parameter tuning is unnecessary. It is found that the following set of values works well for all our experiments $\sigma = 1, T = 0.1, \lambda = 0.5, K = 400$, and B is "Square" with 10 pixels width.

TABLE I
Performance Comparison of Different Features

	[18]	[20]	Ours
Sensitivity	0.87	0.92	0.97
Specificity	0.86	0.88	0.92
Accuracy	0.86	0.90	0.94

A. Evaluation Criteria

The performance of bleeding detection method can be measured with sensitivity, specificity, and accuracy, which are widely used in medical image classification task. They are defined as follows:

$$\begin{aligned} \text{Sensitivity} &= \frac{\text{TP}}{\text{TP}+\text{FN}} \\ \text{Specificity} &= \frac{\text{TN}}{\text{TN}+\text{FP}} \\ \text{Accuracy} &= \frac{\text{TP}+\text{TN}}{\text{TP}+\text{FP}+\text{TN}+\text{FN}} \end{aligned} \tag{6}$$

where TP is the number of positive samples correctly classified. FN is the number of positive samples incorrectly classified as negative. TN is the number of negative samples correctly classified and FP is the number of negative samples incorrectly classified as positive.

High sensitivity means high capability of detecting bleeding frames. High specificity means high capability of avoiding false detection. Accuracy is used to evaluate the overall performance of the proposed method. Since CAD is used to screen for bleeding WCE frames and send them to clinicians for specific examination, sensitivity is more important than specificity and accuracy.

B. Results and Discussions

First, to demonstrate the performance of the proposed color feature, we compared it with the color features used in [18] and [20]. We randomly select 10 000 bleeding pixels and 20 000 nonbleeding pixels from the training set for training and the others for testing. The classification results using SVM are shown in Table I. Apparently, the proposed red ratio feature shows much better discrimination ability for bleeding detection than the other two features.

The left column in Table II shows the detection results of the 5000 WCE images with different basis functions of SVM, such as Linear, Poly, and RBF. It can be observed that all basis functions perform well. Since RBF is the best, we use it to build SVM model in the experiments. Also, to verify the effectiveness of the preprocessing step, we directly use the original image for

TABLE II
BLEEDING DETECTION WITH AND WITHOUT EDGE REMOVAL

	Linear	Poly	RBF
Sensitivity	0.97 / 0.97	0.96 / 0.96	0.99 / 0.99
Specificity	0.89 / 0.83	0.92 / 0.86	0.94 / 0.90
Accuracy	0.91 / 0.86	0.93 / 0.88	0.95 / 0.92

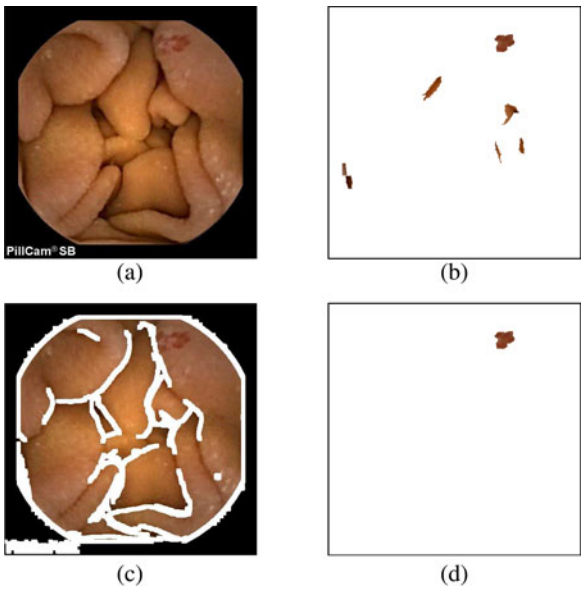

Fig. 4. WCE images. (a) Bleeding image. (b) Detected bleeding regions without edge removal. (c) Edge removal by masking. (d) Detected bleeding regions with edge removal.

TABLE III
PERFORMANCE COMPARISON

	LY	LM	PY	Ours
Sensitivity	0.87	0.91	0.94	0.99
Specificity	0.83	0.88	0.85	0.94
Accuracy	0.84	0.89	0.87	0.95

classification without edge removal. The results are shown in the right column of Table II. Apparently, edge removal is able to improve the specificity and accuracy. Fig. 4 shows an example of bleeding detection with and without edge removal.

Besides, we compared the proposed method with some state-of-the-art methods, such as the image based method [11], the patch based method [24], and the pixel based method [18], which are referred as LY, LM, and PY, respectively. We implemented their algorithms based on the authors' instructions. Some codes such as LBP and PNN are publicly available. The experiments were conducted with the same dataset. We tuned parameters for each of them and use the best one for comparison.

Table III gives the comparisons to some existing methods. We mainly focus on comparison of the sensitivity since it is the most important one for medical classification problem as aforementioned. The pixel based method PY outperforms LY and LM. The image based method LY has the lowest sensitivity. This is because it extracts color features from the whole image. If the bleeding region is too small like in Fig. 1(b), this image will probably be missed. LM is better than LY, since features are extracted from small patches rather than the whole image. There are three main reasons why our method performed the best. First, we use superpixel to segment the image wisely, so high performance as that of pixel based method can be maintained. Second, as aforementioned, our proposed red ratio feature has better performance. Finally, the influence of edge pixels has been removed in our method. Fig. 5 shows some detected bleeding images.

TABLE IV
TIME COST COMPARISON (SECOND PER FRAME)

	LY	LM	PY	Ours
FE	0.0002	0.023	0.0001	0.52
SC	0.0001	0.003	21.4	0.02
Total	0.0003	0.026	21.4	0.54

All the algorithms are implemented using MATLAB on a computer with Intel Core 2 Duo T6500, 2.10 GHz CPUs with 2 GB of RAM. The comparison on time cost is shown in Table IV. Basically, the running time is spent in two aspects: feature extraction (FE) and sample classification. The time cost of training is not considered as it is done off-line. As shown in Table V, the fastest one is LY, an image based method. In LY, each image is represented by one feature vector and the time is mainly spent on FE. PY is the slowest method as it is a pixel based method. Bleeding detection is performed pixel by pixel and FE is not needed. LM is a patch based method and thus the speed is between those of LY and PY. Before FE, the image is first divided into uniform patches. Chromaticity moments and LBP texture features are combined to form a vector to represent a patch. So most time is spent in FE. The proposed method is also a patch based method. Instead of dividing an image uniformly as in the case of LM, a superpixel method is given to group pixels adaptively in nonrectangle shapes based on the content and spatial information. So the complexity is slightly higher than that of LM.

Fig. 6 shows the influence of K on bleeding detection. The smaller the K, the closer the method to an image based method. If $K = 1$, the proposed method is equivalent to an image based approach. Hence, the method has low sensitivity and specificity when K is small. On the other side, the larger the K, the closer the method to a pixel based method. If $K = N$, the proposed method turns into a pixel based method. It is found that 400 is good tradeoff for the WCE images captured by PillCam SB2 with resolution 576×576.

Refer to Fig. 7 for some failure cases. It is found that our method may fail to detect two types of images. One is the image with poor illumination and minor angiodysplasia regions whose hue is similar to normal tissue as shown in Fig. 7(a). The other is the image containing intestinal villi and fluid, which makes the hue of the image dark red as shown in Fig. 7(b).

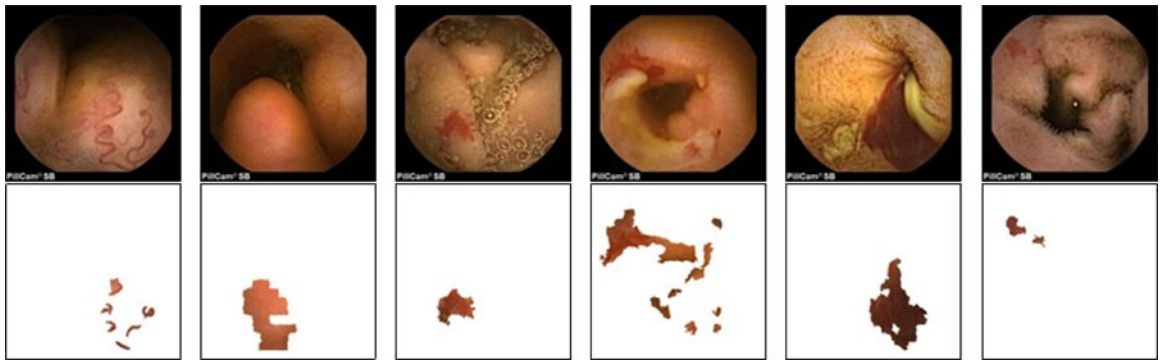

Fig. 5. Detected bleeding images and segmented regions.

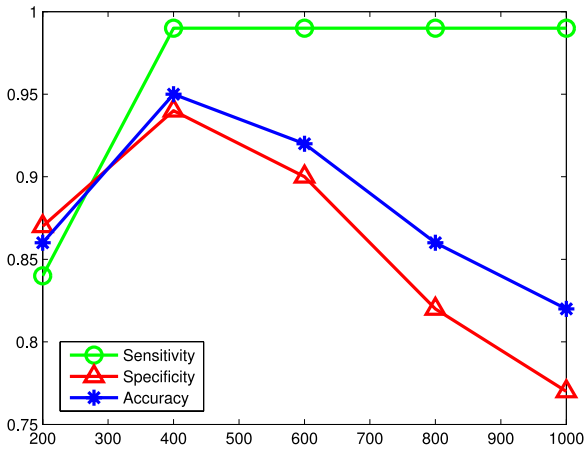

Fig. 6. The influence of K on performance.

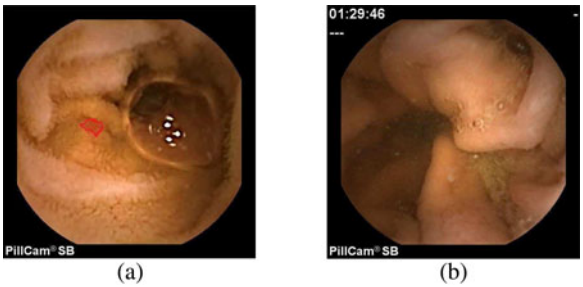

Fig. 7. Failure cases. (a) Missing detection. (b) False detection.

IV. Conclusion

This paper presented a method for bleeding region detection at superpixel level for WCE images. Instead of processing each pixel or dividing the image uniformly, we group pixels adaptively based on color and location through superpixel segmentation. The computational complexity can be reduced a lot compared to pixel based methods while high performance can be maintained. Furthermore, we removed the influence of edge pixels and introduced the red ratio features in the RGB color space, which proved to be better than traditional features on bleeding detection. Experimental results showed that the proposed method outperforms the state-of-the-art methods significantly in terms of sensitivity, specificity, and accuracy.

Acknowledgment

The authors would like to thank Prof. J. Niu of Qilu Hospital of Shandong University who offered plenty of medical instructions and the anonymous reviewers for the comments to improve the quality of this paper. They would also like to thank Given Imaging Ltd. for providing the WCE data (capsuleendoscopy.org).

References

[1] G. Iddan, G. Meron, A. Glukhovsky, and P. Swain, "Wireless capsule endoscopy," *Nature*, vol. 405, p. 417, 2000

[2] A. Ali, J. Santisi, and J. Vargo, "Video capsule endoscopy: A voyage beyond the end of the scope," *Clevel. Clin. J. Med.*, vol. 71, no. 5, pp. 415–425, 2004.

[3] N. Lee and G. Eisen, "10 years of capsule endoscopy: An update," *Expert Rev. Gastroenterol. Hepatol.*, vol. 4, no. 4, pp. 503–512, 2010.

[4] G. Zuckerman, C. Prakash, M. Askin, and B. Lewis, "AGA technical review on the evaluation and management of occult and obscure gastrointestinal bleeding," *Gastroenterology*, vol. 118, no. 1, pp. 201–221, 2000.

[5] A. Karargyris and N. Bourbakis, "Wireless capsule endoscopy and endoscopic imaging: A survey on various methodologies presented," *IEEE Eng. Med. Biol. Mag.*, vol. 29, no. 1, pp. 72–83, Jan./Feb. 2010.

[6] B. Li and M. Meng, "Wireless capsule endoscopy images enhancement via adaptive contrast diffusion," *J. Vis. Commun. Imag. Represent.*, vol. 23, no. 1, pp. 222–228, 2012.

[7] M. Liedlgruber and A. Uhl, "Computer-aided decision support systems for endoscopy in the gastrointestinal tract: A review," *IEEE Rev. Biomed. Eng.*, vol. 4, pp. 73–88, 2011

[8] S. Liangpunsakul, L. Mays, and D. Rex, "Performance of given suspected blood indicator," *Amer. J. Gastroenterol.*, vol. 98, no. 12, pp. 2676–2678, 2003.

[9] J. Rey, "Future perspectives for esophageal and colorectal capsule endoscopy: Dreams or reality?" in *New Challenges in Gastrointestinal Endoscopy.*. Osaka, Japan: Springer, 2008, pp. 55–64.

[10] M. Boulougoura, E. Wadge, V. Kodogiannis, and H. Chowdrey, "Intelligent systems for computer-assisted clinical endoscopic image analysis," in *Proc. 2nd IASTED Int. Conf. Biomed. Eng.*, 2004.

[11] J. Liu and X. Yuan, "Obscure bleeding detection in endoscopy images using support vector machines," *Opt. Eng.*, vol. 10, no. 2, pp. 289–299, 2009.

[12] M. Coimbra and J. Cunha, "MPEG-7 visual descriptors contributions for automated feature extraction in capsule endoscopy," *IEEE Trans. Circuits Syst. Video Technol.*, vol. 16, no. 5, pp. 628–637, May 2006.

[13] B. Li and M. Q.-H. Meng, "Texture analysis for ulcer detection in capsule endoscopy images," *Imag. Vis. Comput.*, vol. 27, no. 9, pp. 1336–1342, 2009.

[14] B. Giritharan, X. Yuan, J. Liu, B. Buckles, J. Oh, and S. Tang, "Bleeding detection from capsule endoscopy videos," in *Proc. 30th Annu. Int. Conf. IEEE Eng. Med. Biol. Soc.*, Aug. 2008, pp. 4780–4783.

[15] P. Khun, Z. Zhuo, L. Yang, L. Liyuan, and L. Jiang, "Feature selection and classification for wireless capsule endoscopic frames," in *Proc. Int. Conf. Biomed. Pharmaceut. Eng.*, Dec. 2009, pp. 1–6.
[16] B. Li, M. Meng, and J. Lau, "Computer-aided small bowel tumor detection for capsule endoscopy," *Artif. Intell. Med.*, vol. 52, no. 1, pp. 11–16, 2011.
[17] B. Li and M. Meng, "Tumor recognition in wireless capsule endoscopy images using textural features and SVM-based feature selection," *IEEE Trans. Inform. Technol. Biomed.*, vol. 16, no. 3, pp. 323–329, May 2012.
[18] G. Pan, G. Yan, X. Qiu, and J. Cui, "Bleeding detection in wireless capsule endoscopy based on probabilistic neural network," *J. Med. Syst.*, vol. 35, no. 6, pp. 1477–1484, 2011.
[19] A. A. Al-Rahayfeh and A. A. Abuzneid, "Detection of bleeding in wireless capsule endoscopy images using range ratio color," *Int. J. Multimedia Appl.*, vol. 2, no. 2, pp. 1–10, 2010.
[20] S. Hwang, J. Oh, J. Cox, S. Tang, and H. Tibbals, "Blood detection in wireless capsule endoscopy using expectation maximization clustering," in *Proc. SPIE*, vol. 6144, pp. 1–11, 2006.
[21] B. Penna, T. Tillo, M. Grangetto, E. Magli, and G. Olmo, "A technique for blood detection in wireless capsule endoscopy images," in *Proc. 17th Eur. Signal Process. Conf.*, Glasgow, Scotland, 2009, pp. 1864–1868.
[22] Y. Jung, Y. Kim, D. Lee, and J. Kim, "Active blood detection in a high resolution capsule endoscopy using color spectrum transformation," in *Proc. Int. Conf. Biomed. Eng. Inf.*, May 2008, vol. 1, pp. 859–862.
[23] P. Lau and P. Correia, "Detection of bleeding patterns in wce video using multiple features," in *Proc. IEEE 29th Annu. Int. Conf. Eng. Med. Biol. Soc.*, Aug. 2007, pp. 5601–5604.
[24] B. Li and M. Meng, "Computer-aided detection of bleeding regions for capsule endoscopy images," *IEEE Trans. Biomed. Eng.*, vol. 56, no. 4, pp. 1032–1039, Apr. 2009.
[25] Y. Fu, M. Mandal, and G. Guo, "Bleeding region detection in wce images based on color features and neural network," in *Proc. IEEE 54th Int. Midwest Symp. Circuits Syst.*, Aug. 2011, pp. 1–4.
[26] J. Canny, "A computational approach to edge detection," *IEEE Trans. Patt. Anal. Mach. Intell.*, vol. 8, no. 6, pp. 679–698, Nov. 1986.
[27] R. C. Gonzalez and R. E. Woods, *Digital Image Processing,*, 3rd ed. Upper Saddle River, NJ, USA: Prentice-Hall, 2006.
[28] X. Ren and J. Malik, "Learning a classification model for segmentation," in *Proc. IEEE 9th Int. Conf. Comput. Vis.*, Oct. 2003, vol. 1, pp. 10–17.
[29] A. Levinshtein, A. Stere, K. Kutulakos, D. Fleet, S. Dickinson, and K. Siddiqi, "Turbopixels: Fast superpixels using geometric flows," *IEEE Trans. Patt. Anal. Mach. Intell.*, vol. 31, no. 12, pp. 2290–2297, Dec. 2009.
[30] R. Achanta, A. Shaji, K. Smith, A. Lucchi, P. Fua, and S. Susstrunk, "Slic superpixels compared to state-of-the-art superpixel methods," *IEEE Trans. Patt. Anal. Mach. Intell.*, vol. 34, no. 11, pp. 2274–2282, Nov. 2012.
[31] C.-C. Chang and C.-J. Lin, "LIBSVM: A library for support vector machines," *ACM Trans. Intell. Syst. Technol.*, vol. 2, pp. 27:1–27:27, 2011.
[32] J. Berens, G. Finlayson, and G. Qiu, "Image indexing using compressed colour histograms," *IEE Proc. Vis. Imag. Signal Process.*, vol. 147, no. 4, pp. 349–355, Aug. 2000.

Yanan Fu (S'10) received the Bachelor's degree in biomedical engineering and the Master's degree in system engineering both from Shandong University, Jinan, China, in 2004 and 2007, respectively. He is currently working toward the Ph.D. degree in biomedical engineering in the Department of Control Science and Engineering, Shandong University. His current research interests include medical and diagnostic imaging.

Wei Zhang (S'06–M'11) received the B.E. degree in automation and the M.E. degree in electronic engineering from Anhui University, Hefei, China, in 2003 and 2006, respectively, and the Ph.D. degree in electronic engineering from The Chinese University of Hong Kong, Shatin, Hong Kong, in 2010.

He is currently with the School of Control Science and Engineering, Shandong University, Jinan, China. His research interests include image processing, computer vision, biomedical engineering, and robotics. He has published more than 20 papers in prestigious journals and refereed conferences. He served as a Program Committee Member and Reviewer for various international conferences and journals in image processing, computer vision, and biomedical engineering.

Mrinal Mandal (M'99–SM'03) received the B.E. degree in electronics and communication engineering from the National Institute of Technology, Durgapur, India, and the M.A.Sc. and Ph.D. degrees in electrical and computer engineering from the University of Ottawa, Canada.

He is currently a Professor and Associate Chair in the Department of Electrical and Computer Engineering and is the Director of the Multimedia Computing and Communications Laboratory, the University of Alberta, Edmonton, AB, Canada. He has authored the book *Multimedia Signals and Systems* (Norwell, MA, USA: Kluwer, 2003), and co-authored the book *Continuous and Discrete Time Signals and Systems,* (Cambridge, U.K.: Cambridge Univ. Press, 2007). His current research interests include multimedia, image and video Processing, multimedia communications, medical image analysis. He has published more than 150 papers in refereed journals and conferences, and has a U.S. patent on lifting wavelet transform architecture. He has been the Principal Investigator of projects funded by Canadian Networks of Centers of Excellence such as CITR and MICRONET, and is currently the Principal Investigator of a project funded by the NSERC. He received the Canadian Commonwealth Fellowship and Humboldt Research Fellowship (Germany).

Max Q.-H. Meng (M'92–F'08) received the Master's degree from Beijing Institute of Technology, Beijing, China, in 1988, and the Ph.D. degree in electrical and computer engineering from the University of Victoria, BC, Canada, in 1992.

He has been a Professor of electronic engineering at the Chinese University of Hong Kong, Hong Kong, since August 2002. He was with the University of Alberta in Canada as an Assistant Professor in 1994, an Associate Professor in 1998, and a Professor in 2000, respectively. His research interests include medical robotics and devices. He has published over 450 international journal and conference papers. He served as an Associate VP for Conferences of the IEEE Robotics and Automation Society and an Ad Com member of the IEEE Neural Network Council/Society. He received the IEEE Third Millennium Medal Award.